



EGU2020-2273



Chat time: Tue, 05 May, 08:30–10:15

# Extension discrepancy distribution of the hyper-thinned continental crust in the Baiyun Rift, northern margin of the South China Sea

---

**Yanghui Zhao<sup>1</sup>, Weiwei Ding<sup>1</sup>, Jianye Ren<sup>2</sup>, Jiabiao Li<sup>1</sup>, Dianjun Tong<sup>2</sup>, Jiangyang Zhang<sup>3</sup>**

<sup>1</sup>Second Institute of Oceanography, Ministry of Natural Resources, Hangzhou, China

<sup>2</sup>College of Marine Science and Technology, China University of Geosciences, Wuhan, China

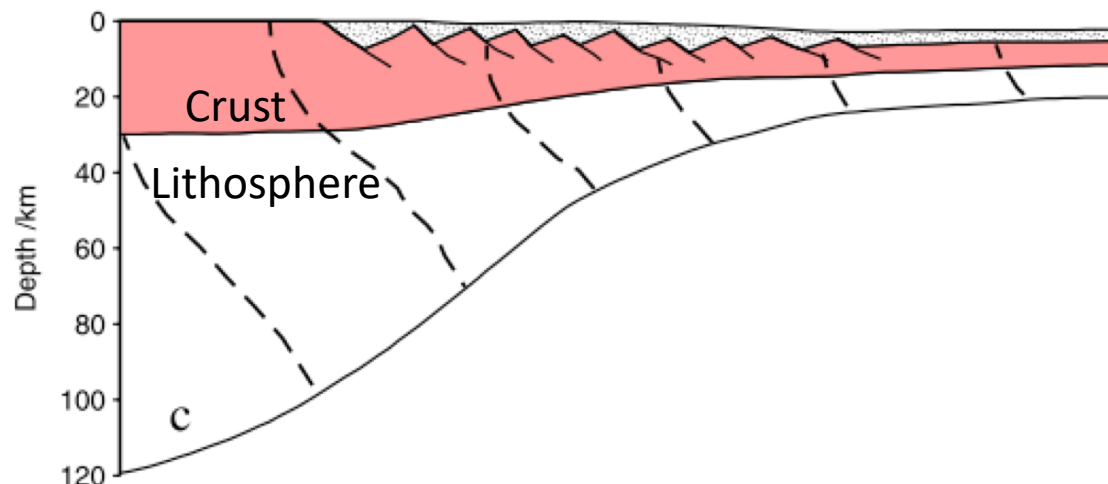
<sup>3</sup>Shenzhen Research Institute, Chinese University of Hong Kong, Shenzhen, China



Email: [zhaoyh@sio.org.cn](mailto:zhaoyh@sio.org.cn)

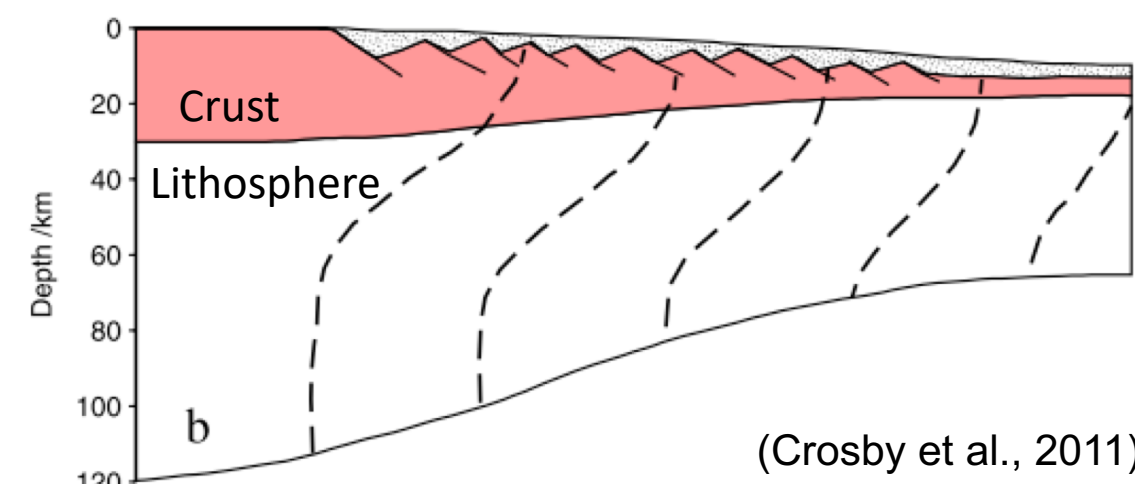
## Scenario A

Lithospheric mantle is thinned more than crust



## Scenario B

Crust is thinned more than lithospheric mantle



(Crosby et al., 2011)

**Extension discrepancy**, upper crust thinned far less than whole crust or lithosphere.

- North Sea (Ziegler, 1983; White 1990)
- Norwegian rifted margin (Kusznir et al., 2005)
- Brazil-Angolan margins (Moulin et al., 2005)

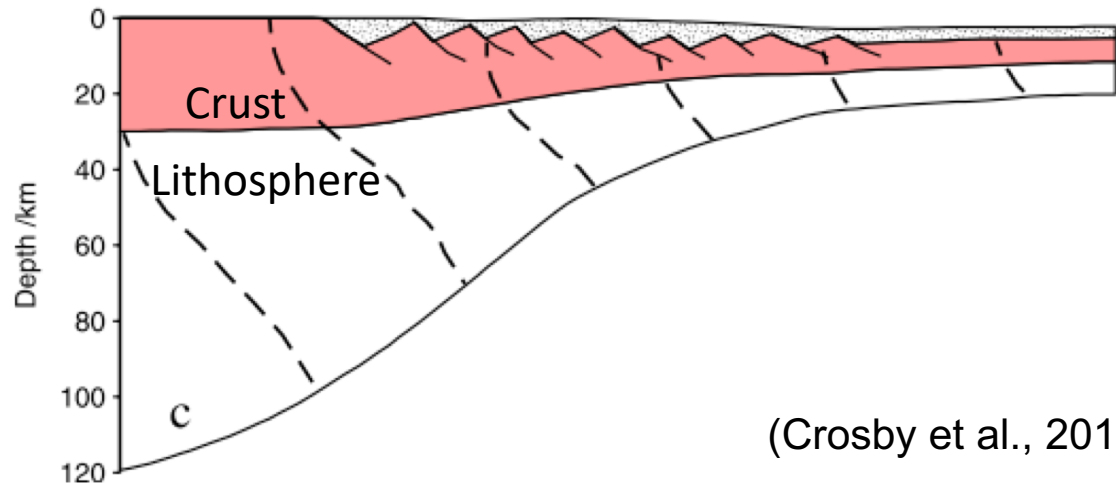
**Inverse extension discrepancy**, in the hyper-extended domain of rifted margins, the upper crustal extension could exceed the whole crust.

- Brazil-Angolan margin (Crosby et al., 2011)
- Galicia margin (McDermott & Reston, 2015).

## Background

### Scenario A

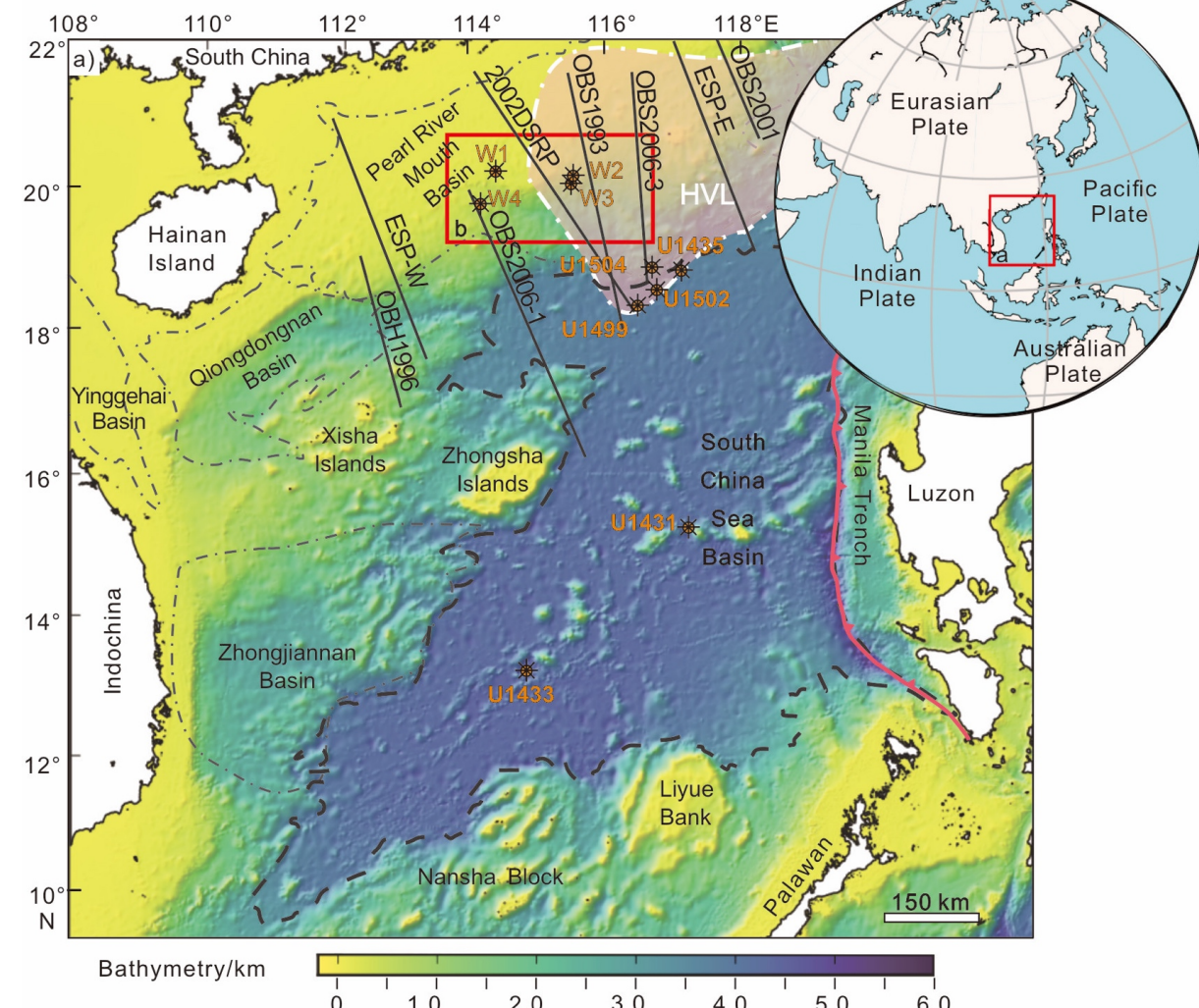
Lithospheric mantle is thinned more than crust



(Crosby et al., 2011)

In the South China Sea margins, most studies reported  
**extension discrepancy**

- Pearl River Mouth basin (Bai et al., 2019; Clift et al., 2002; Hsu et al., 2004)
- Qiongdongnan basin (Tong et al., 2009; Zhao Z. et al., 2018)
- Northwest Palawan margin (Franke et al., 2011)
- Offshore Vietnam (Savva et al., 2014)



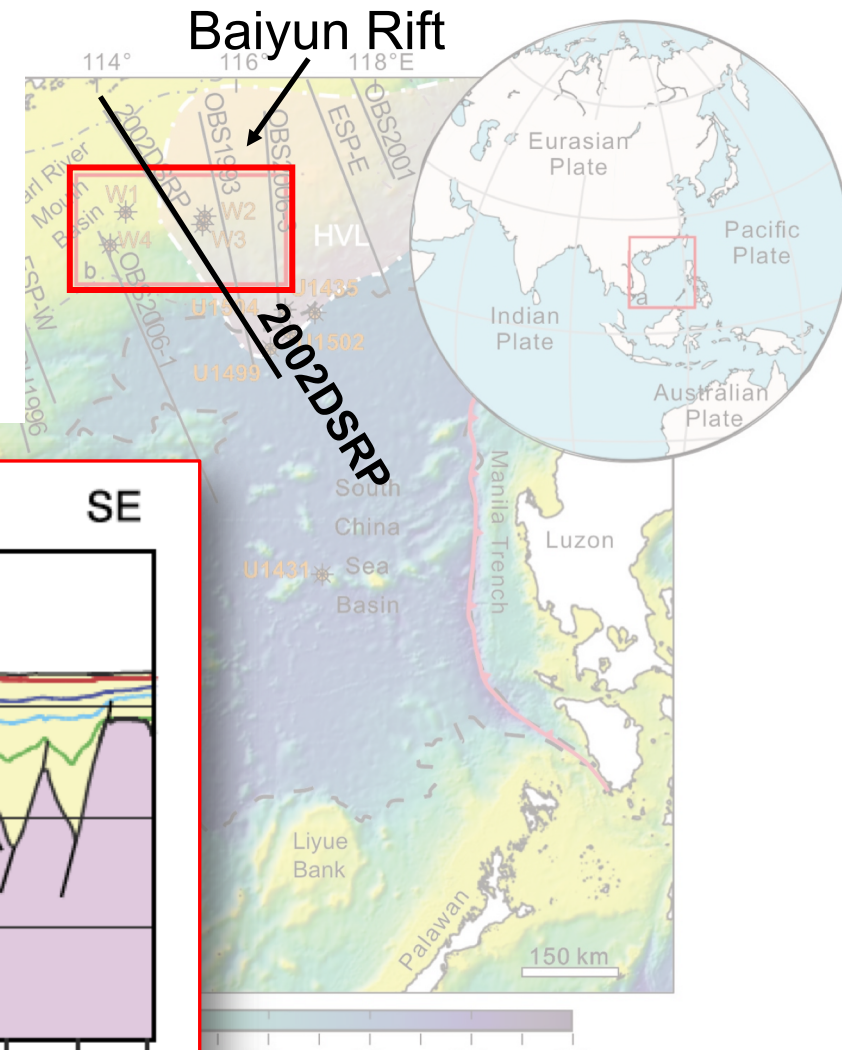
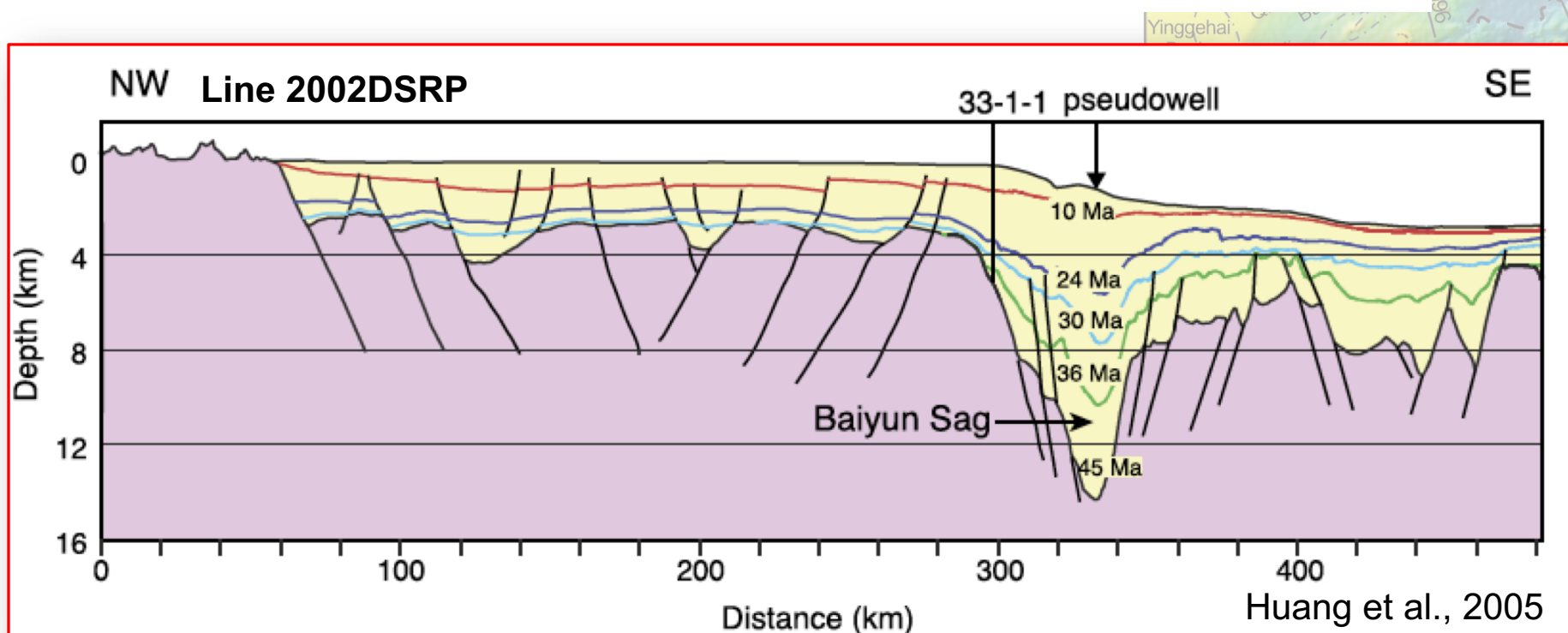
HVL: high-velocity layer in the lower crust

(Zhao Y. et al, 2020, under review)

## Background

However, previous studies may have underestimated upper crustal thinning:

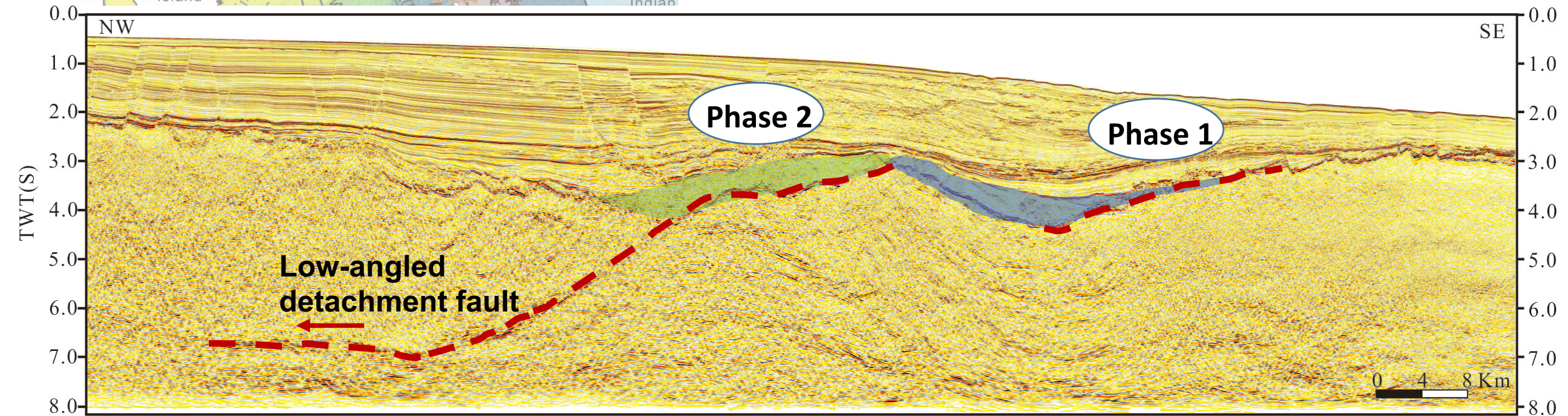
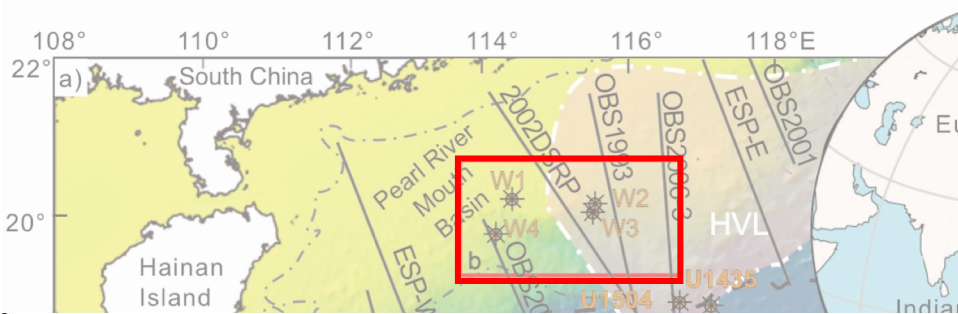
- 1) based on a classic rifted basin model that the rifting was controlled continuously by **high-angle normal faulting**,
- 2) under an assumption that the **observed faulting is close to the total amount of brittle extension**.



## Background

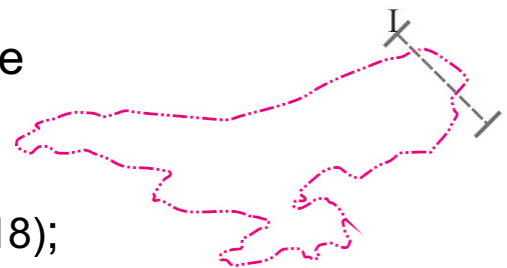
---

### Baiyun Rift



Newly acquired high-resolution multi-channel seismic data indicate that the faults in the hyper-extended domain of the Northern South China Sea show:

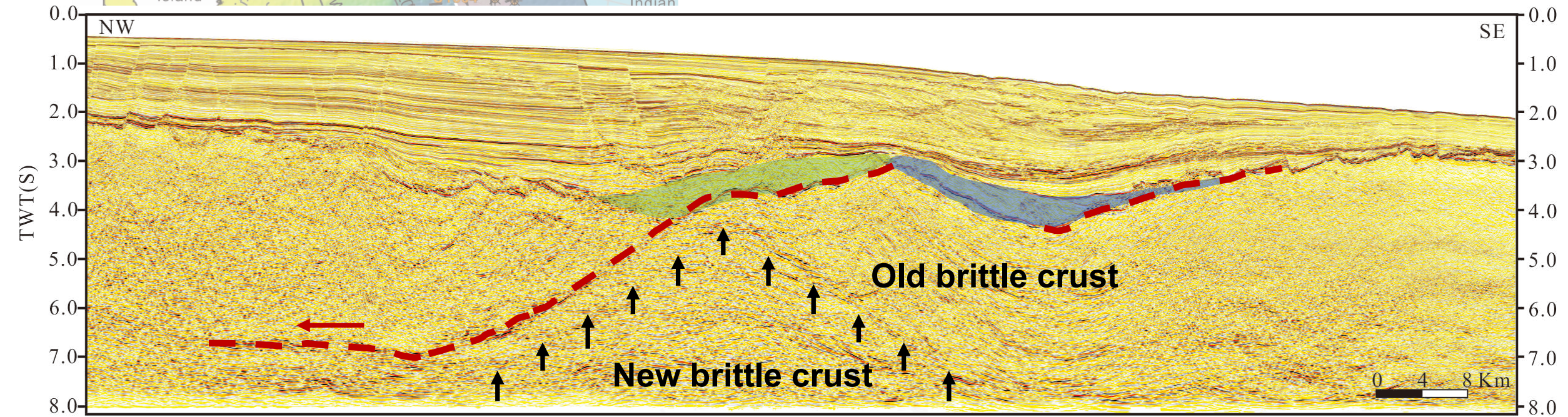
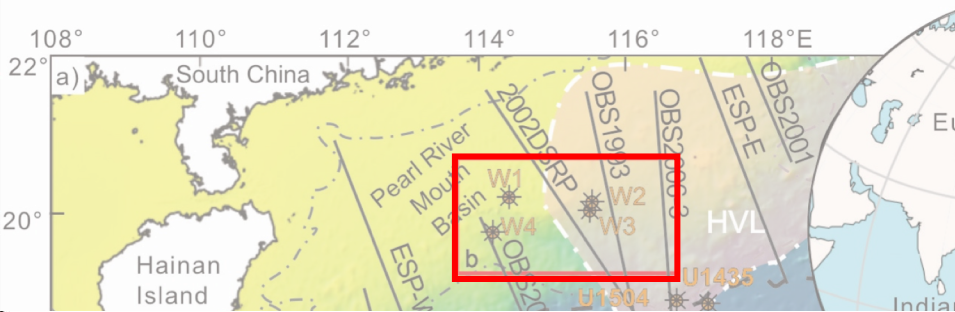
- 1) **Low-angled detachment fault** dominated the rifted basin evolution (Zhao Y. et al., 2018);
- 2) **Polyphase faulting** was failed to restored in previous studies;



## Background

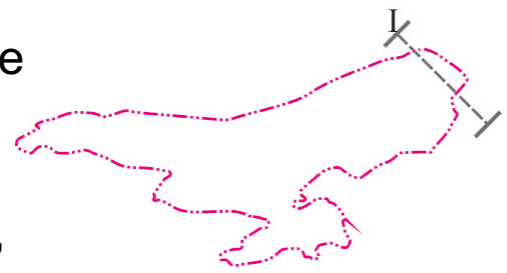
---

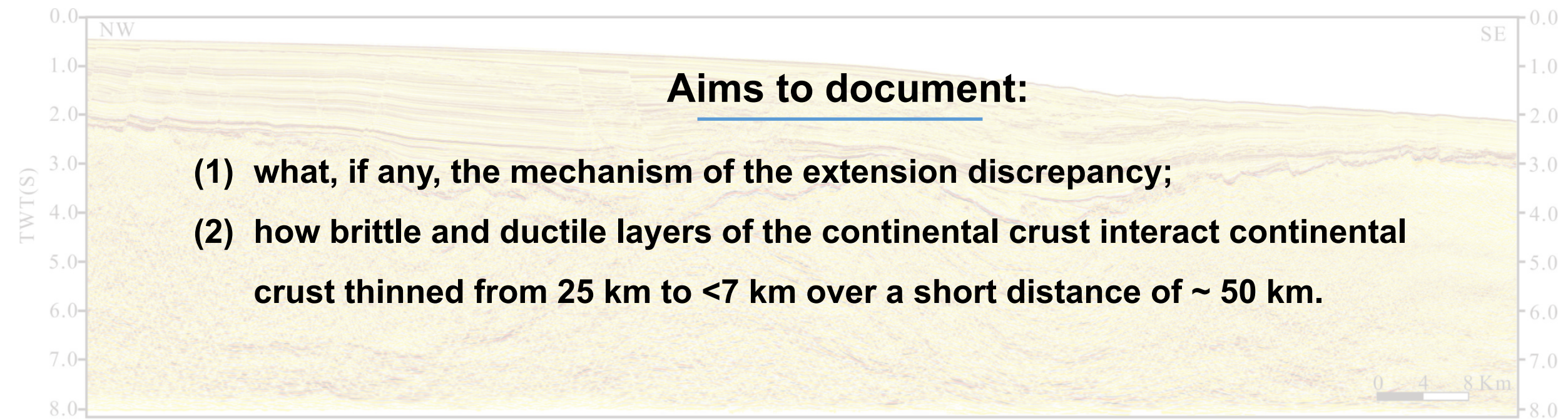
### Baiyun Rift



Newly acquired high-resolution multi-channel seismic data indicate that the faults in the hyper-extended domain of the Northern South China Sea show:

- 3) **Lower crustal exhumation** formed a new brittle crust during the detachment faulting, which may result in uncertainties of crustal stretching factor.





## 1. Seismic interpretation

- Using basin-covered 3D seismic data
- Sedimentary basin structure
- Crustal structure

## 2. Time-depth conversion

- Stratigraphic velocity after 41 drilling wells
- Crustal velocity after seismic modeling of OBS profiles

## 3. Rift structure restoration

- Software Move (Midland Valley)
- Following areal balancing principle

## 4. Crustal extension quantification

- Crustal thinning factor
- Fault-derived stretching factor
- Sub-resolution faulting examination

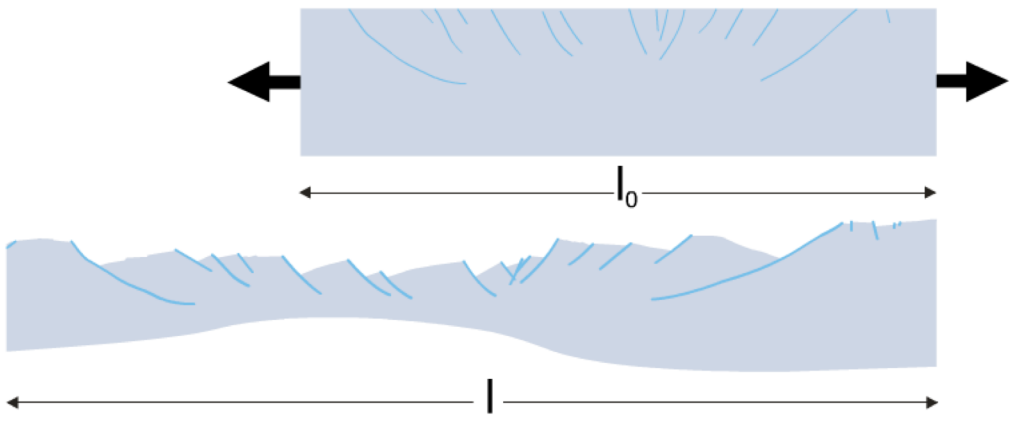


## Two methods to quantify crustal stretching/thinning amount:

#1, stretching factor,  $\gamma_f$

$$\beta_f = \left(1 + \beta_0 \cos^2 \left[ \frac{\pi(x-x_0)}{W} \right]\right)$$

To represent graphically,  $\gamma_f = 1 - 1/\beta_f$



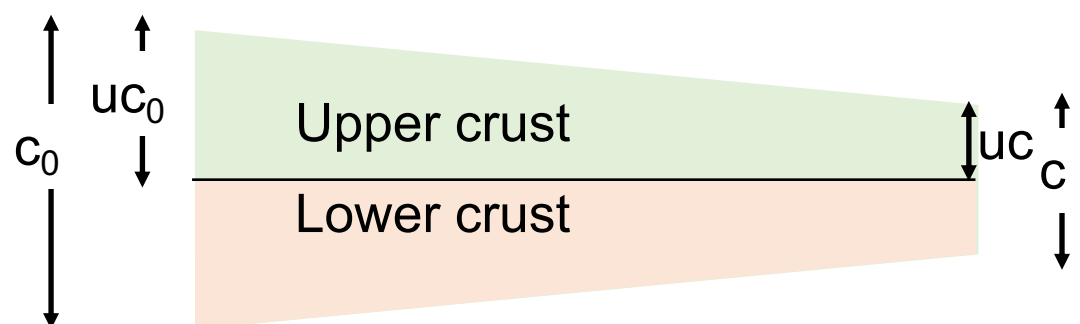
#2, Crustal thinning factor,  $\gamma_{uc}$  and  $\gamma_c$

$$\beta_{uc} = Z_{uc0}/Z_{uc} \quad (\text{theoretically } = \beta_f)$$

$$\beta_c = Z_{c0}/Z_c$$

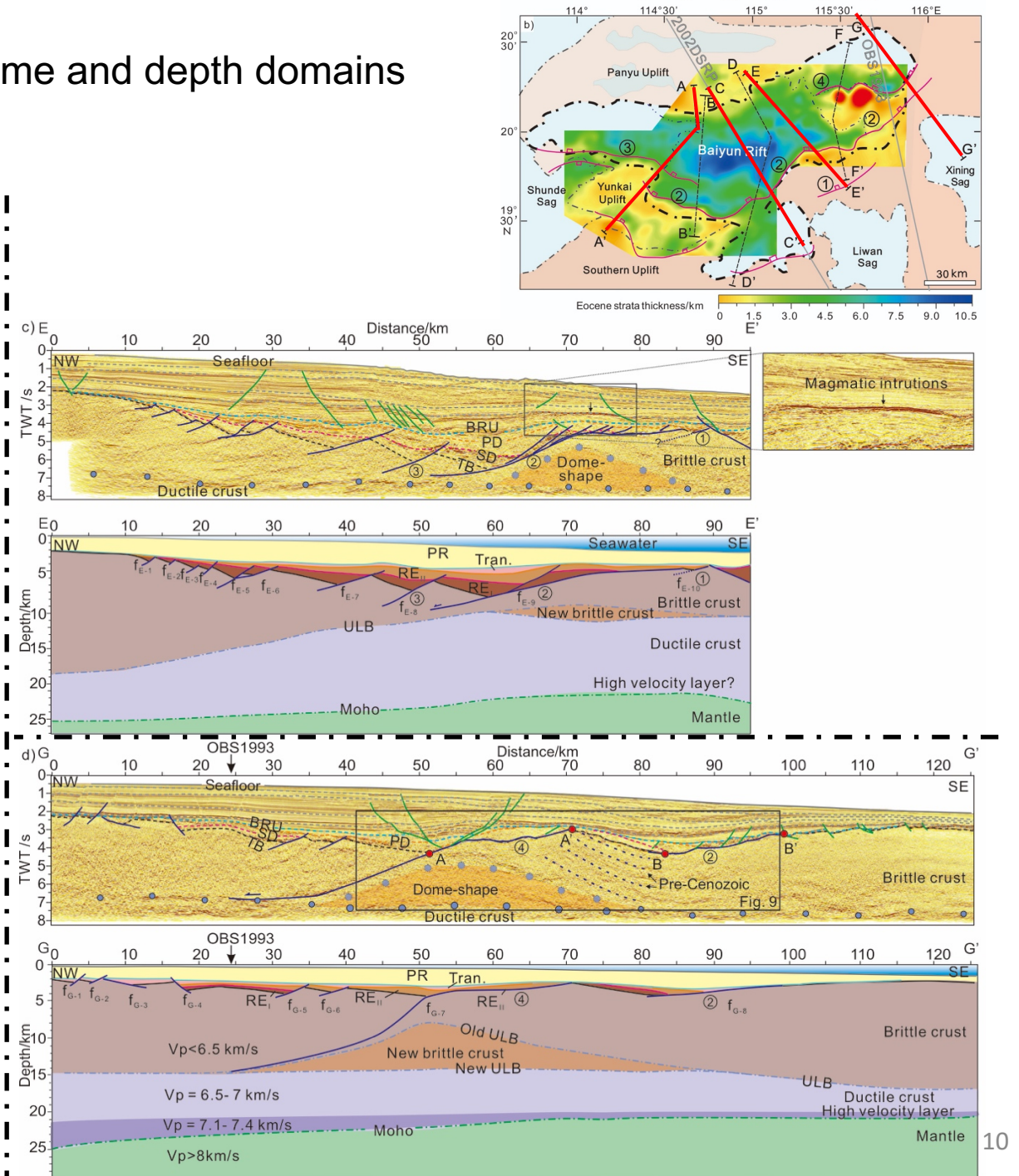
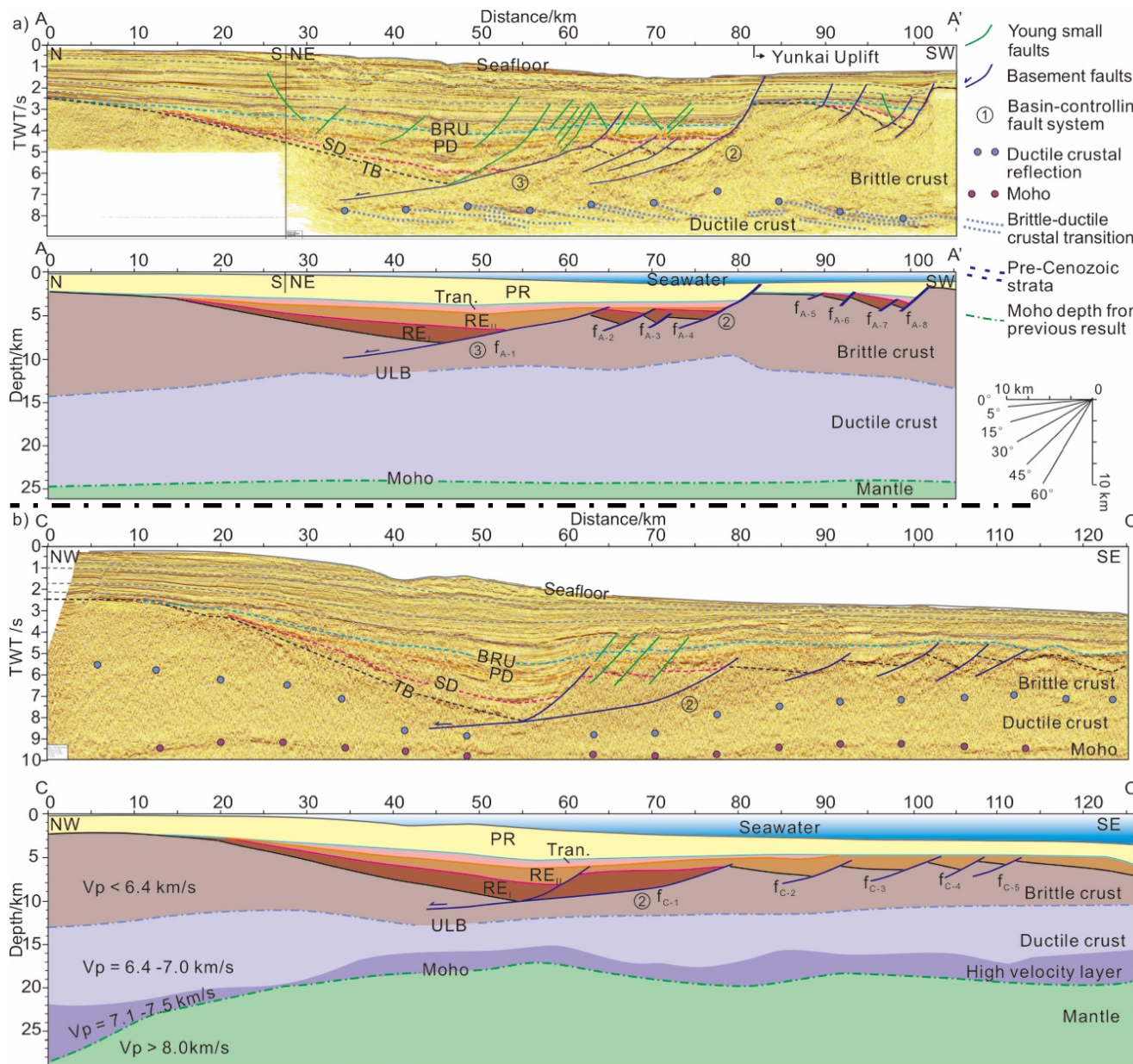
To represent graphically,  $\gamma_{uc} = 1 - 1/\beta_{uc}$

$$\gamma_c = 1 - 1/\beta_c$$



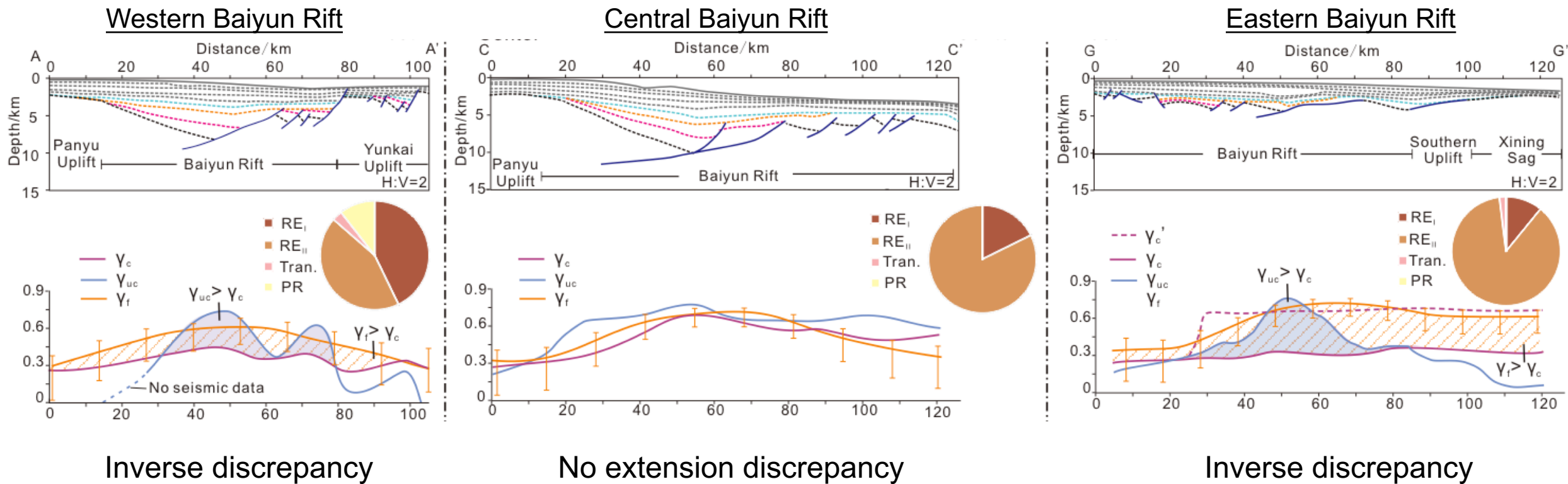
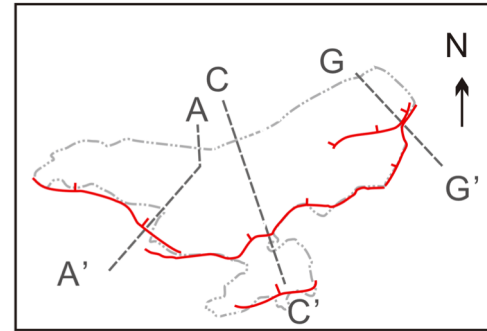
# Results

## — Interpretations of seismic sections in time and depth domains See notes at end of presentation.



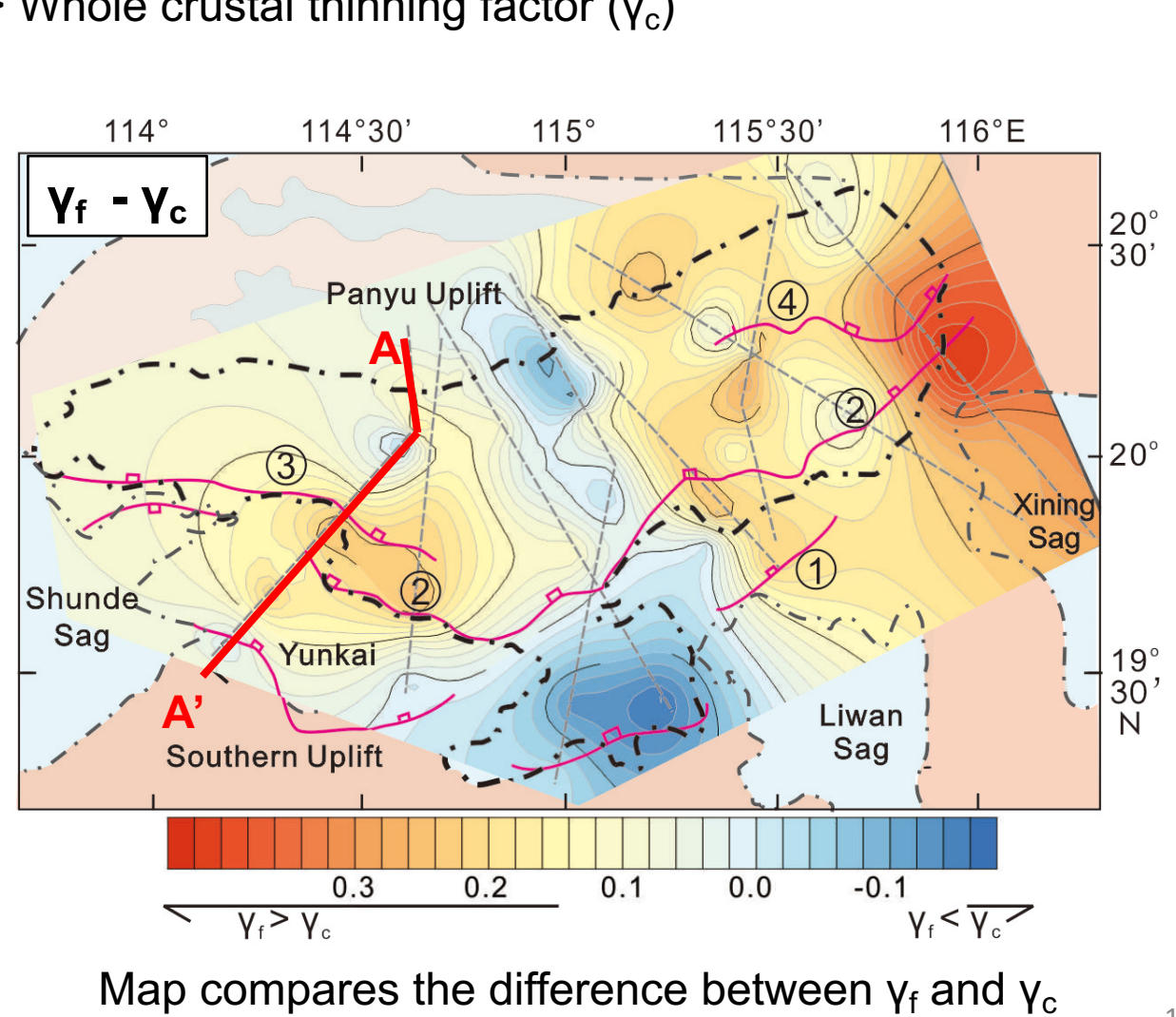
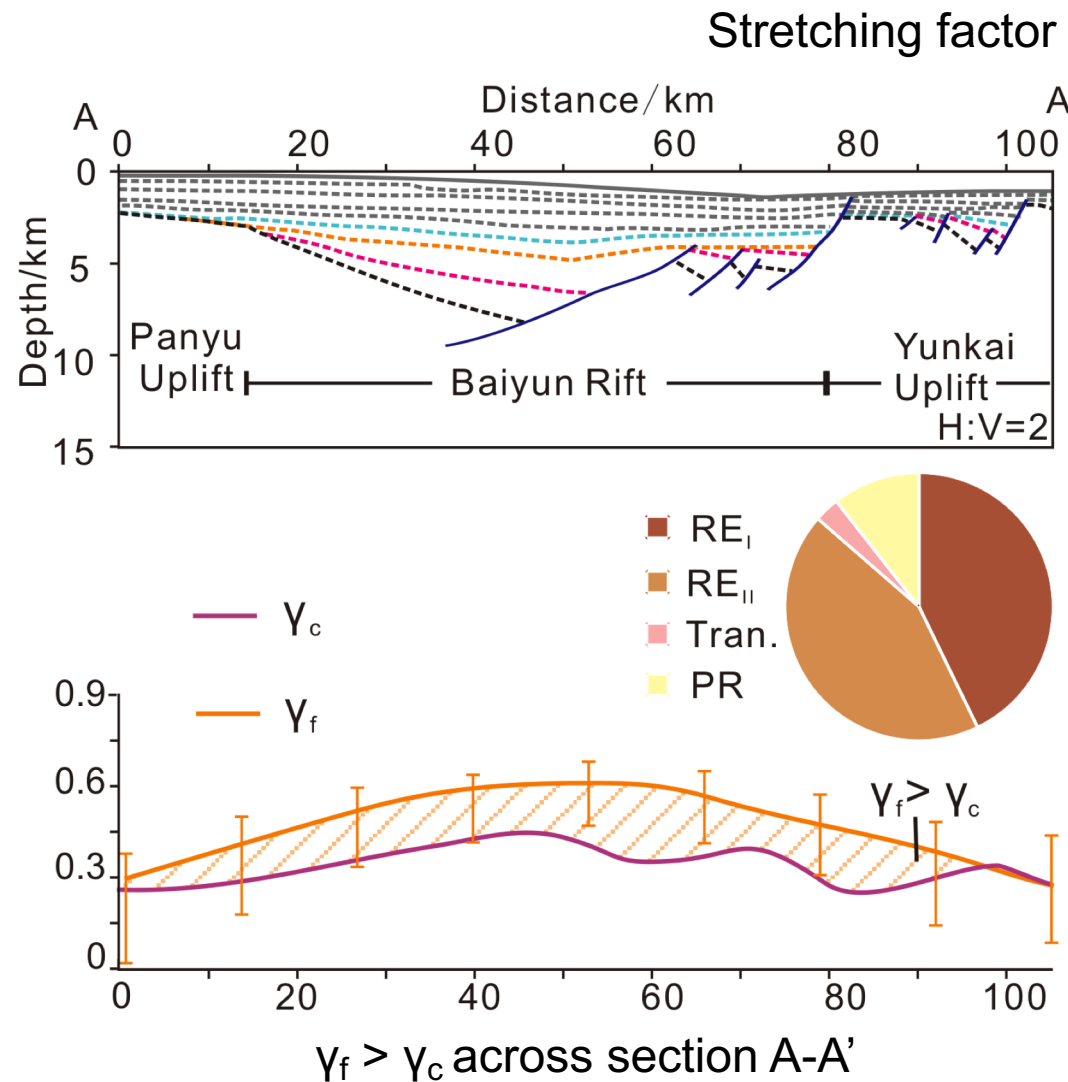
# Results

— Selected depth sections and the comparisons between whole crustal thinning factor ( $\gamma_c$ ), upper crustal thinning factor ( $\gamma_{uc}$ ), and stretching factor ( $\gamma_f$ ).  
See notes at end of presentation.



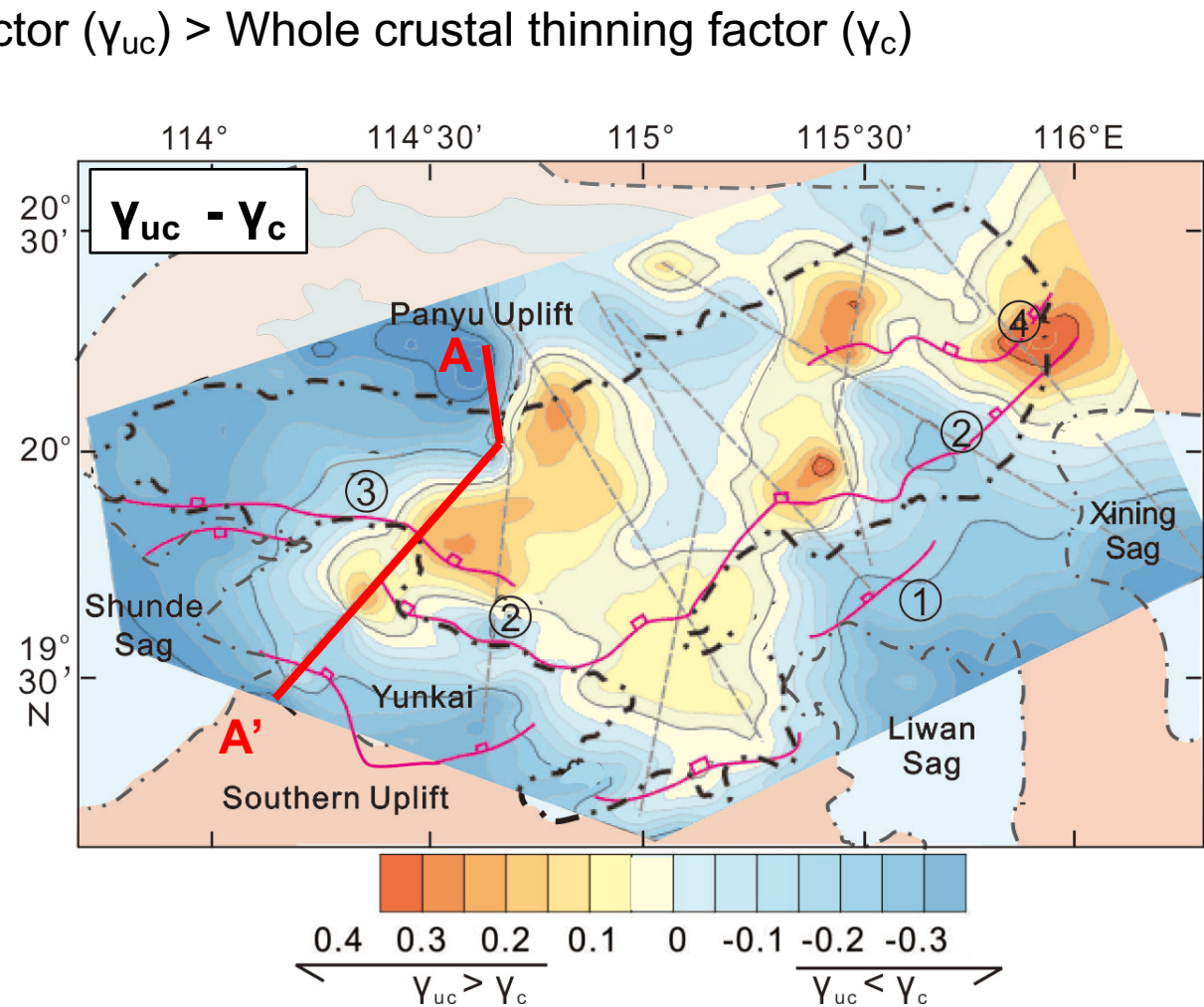
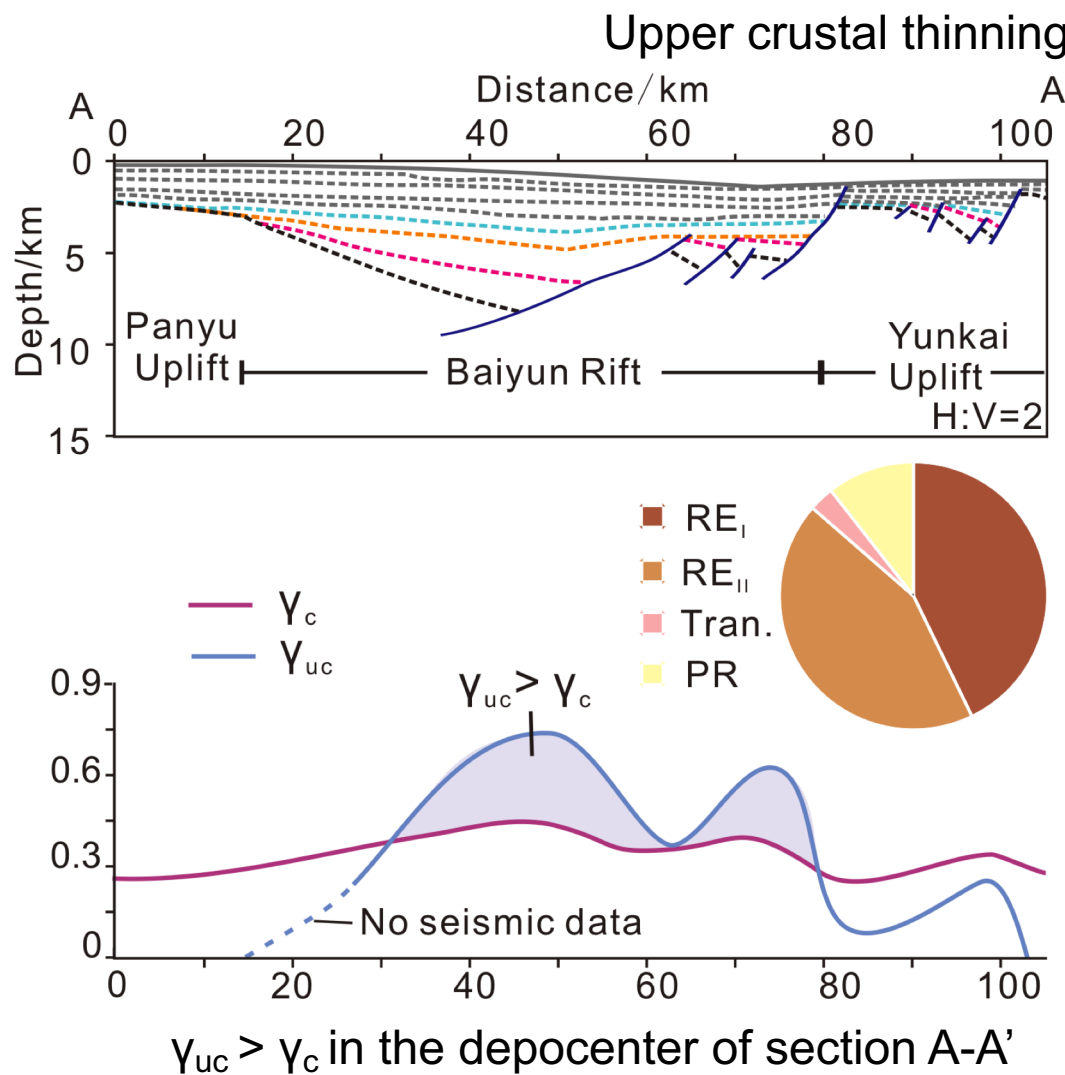
# Western Baiyun Rift

Inverse discrepancy



# Western Baiyun Rift

## Inverse discrepancy



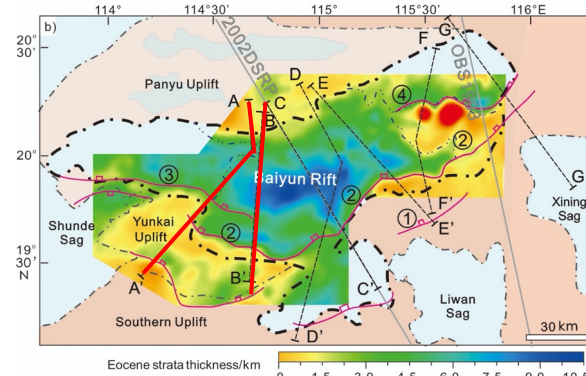
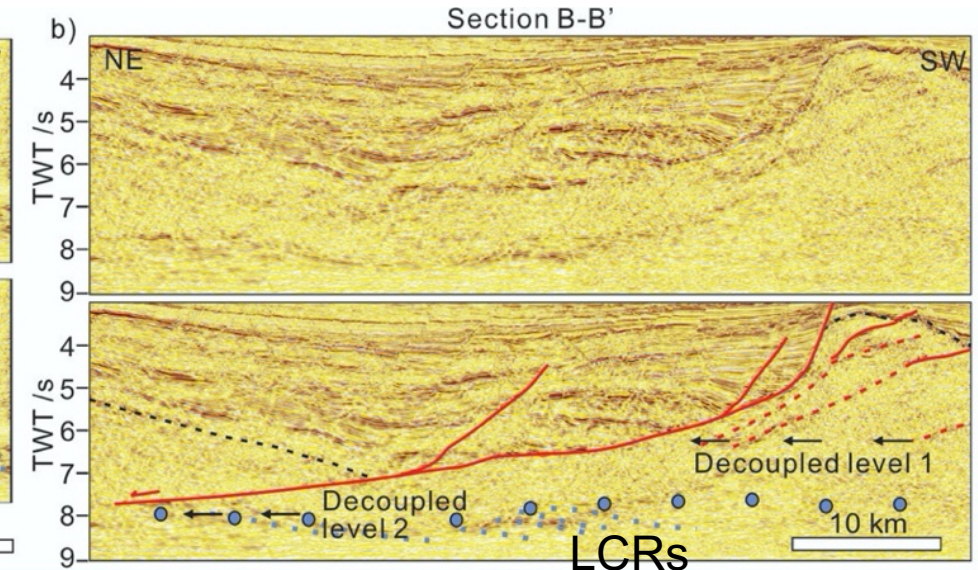
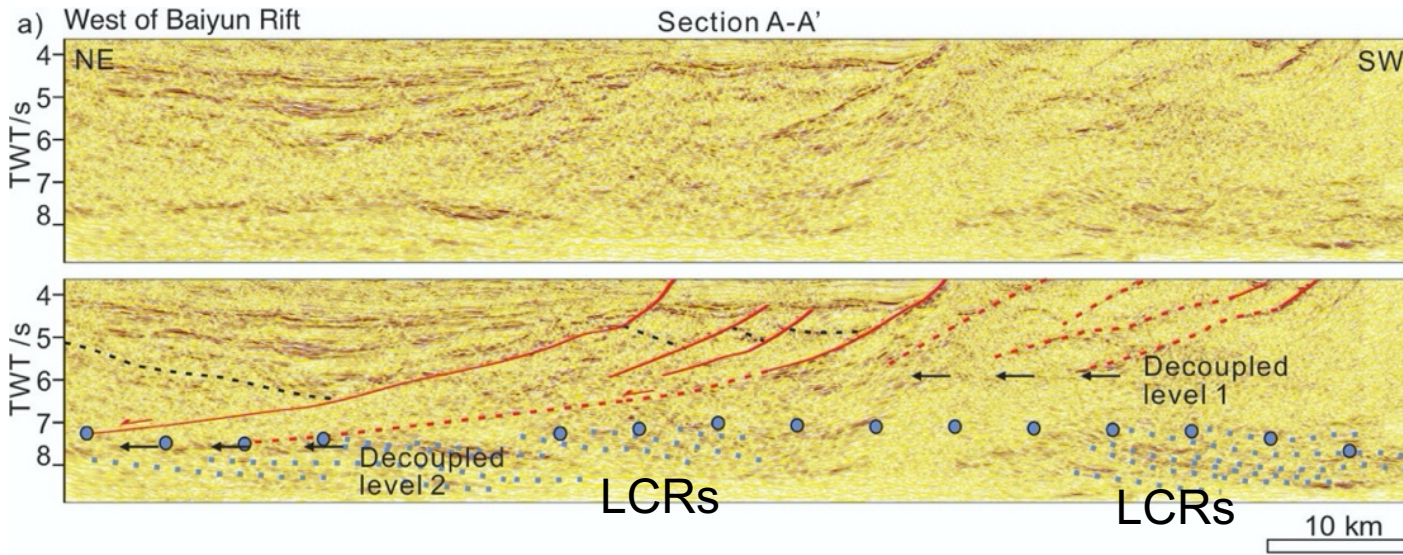
Map compares the difference between  $\gamma_{uc}$  and  $\gamma_c$

# Western Baiyun Rift

Possible cause: ductile shearing deformation

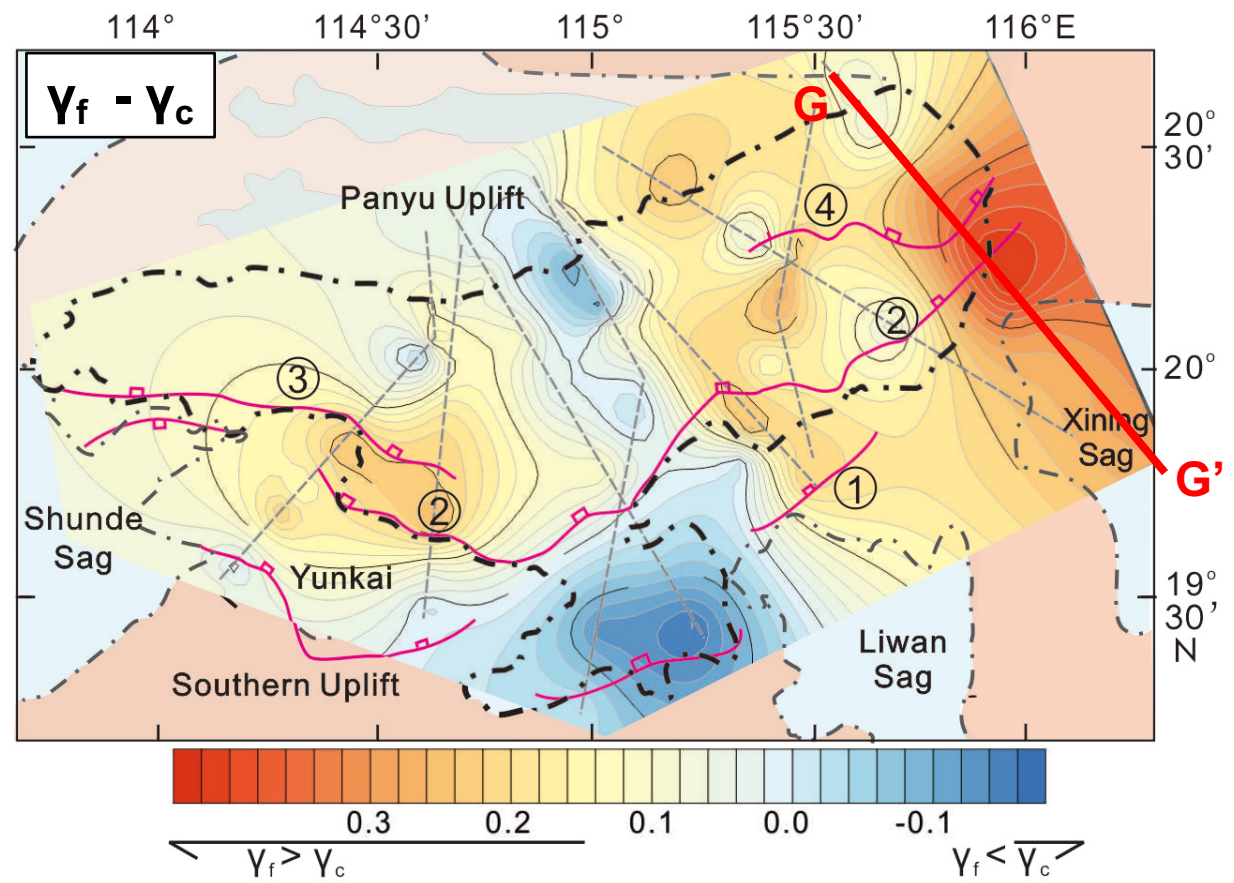
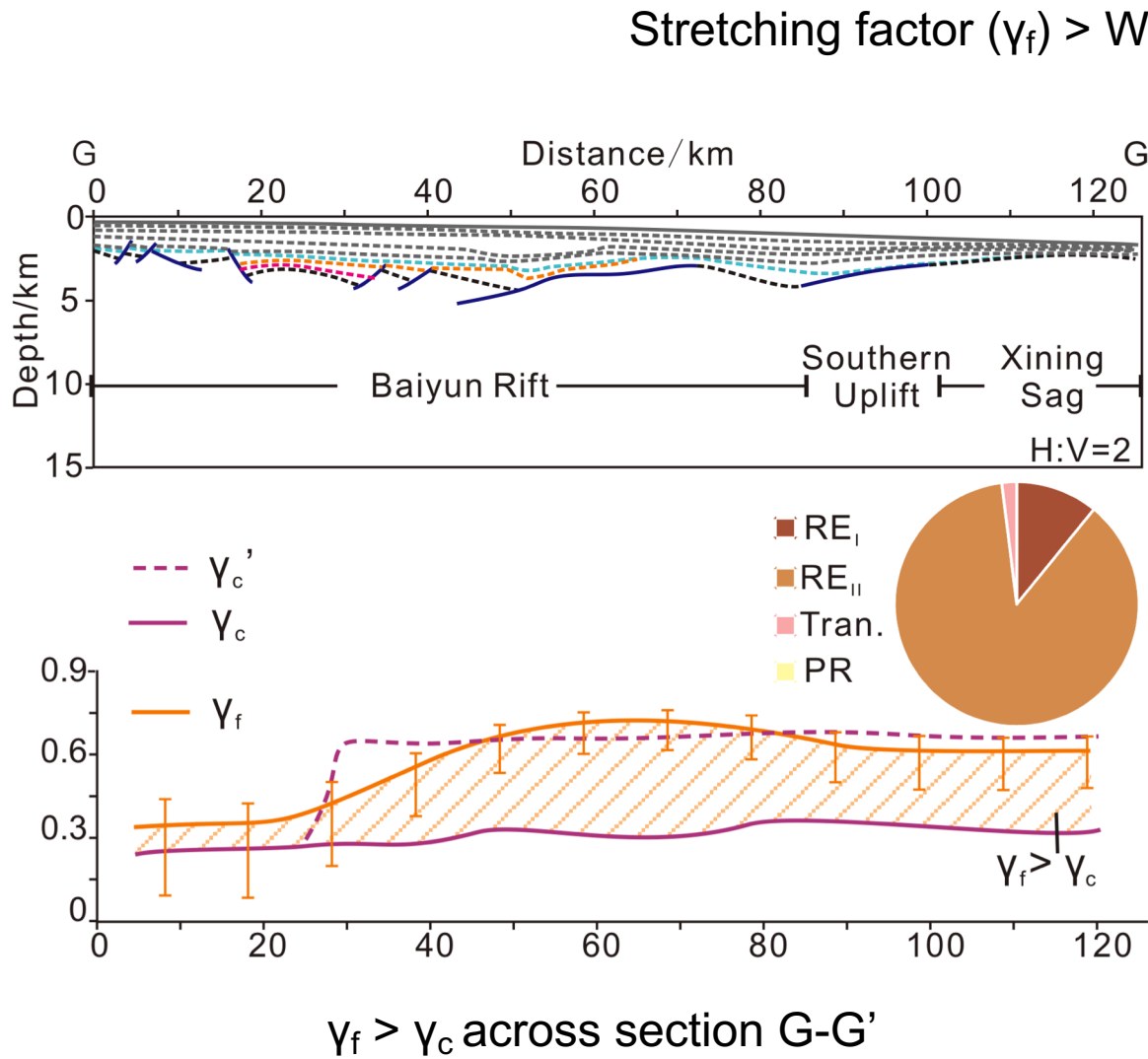
**Evidence** In the western Baiyun Rift, lower crustal reflections (LCRs) are identified near the brittle-ductile transition. These LCRs are symmetric to the continentward-dipping faults and notably abundant beneath the low-angled normal faults (LANFs) reflections, which indicates a deformation dominated by a simple shear towards the continent.

Hence, inverse discrepancy in the western Baiyun Rift is achieved by an intense tectonic faulting in the upper crust and a relatively weak ductile shearing in the lower crust.



# Eastern Baiyun Rift

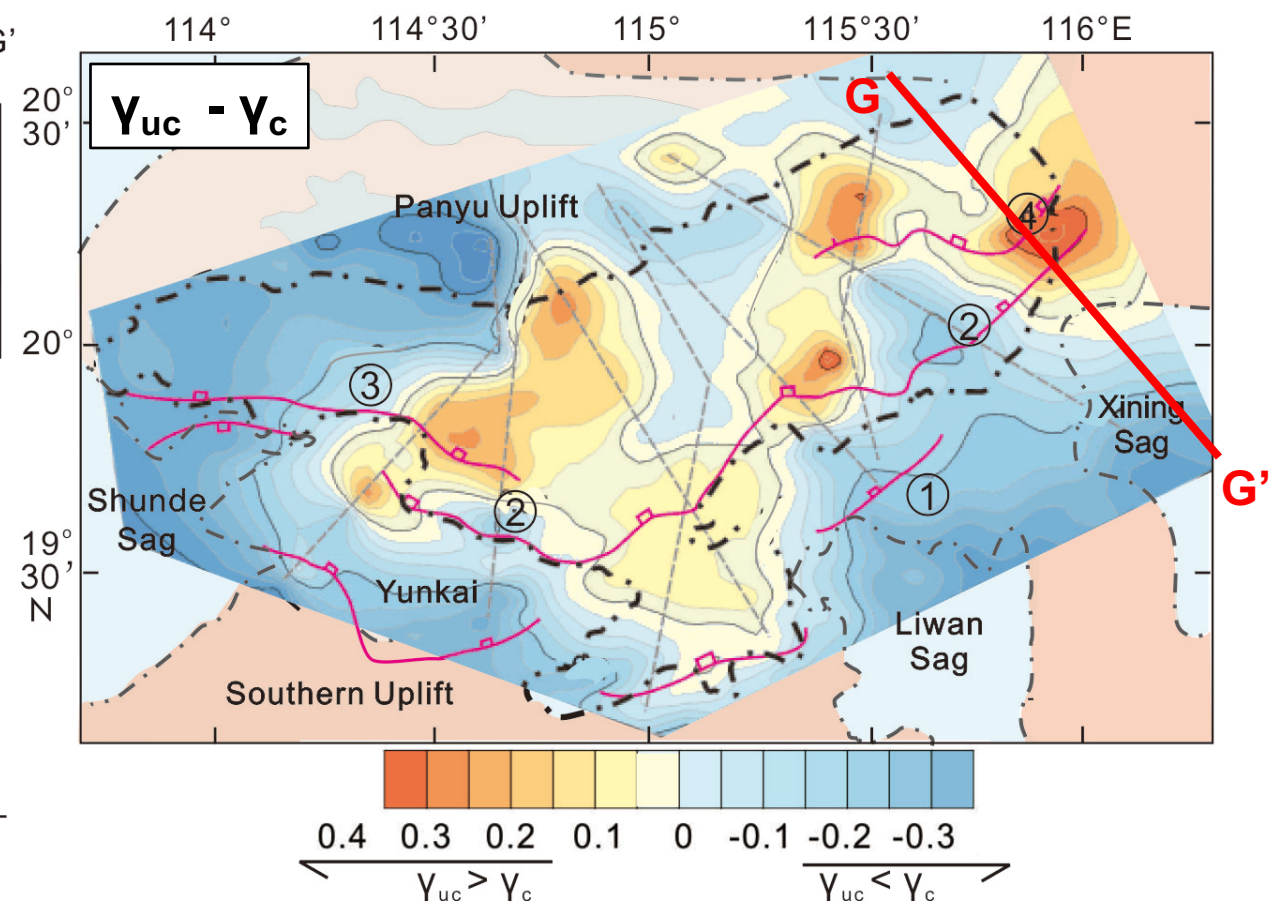
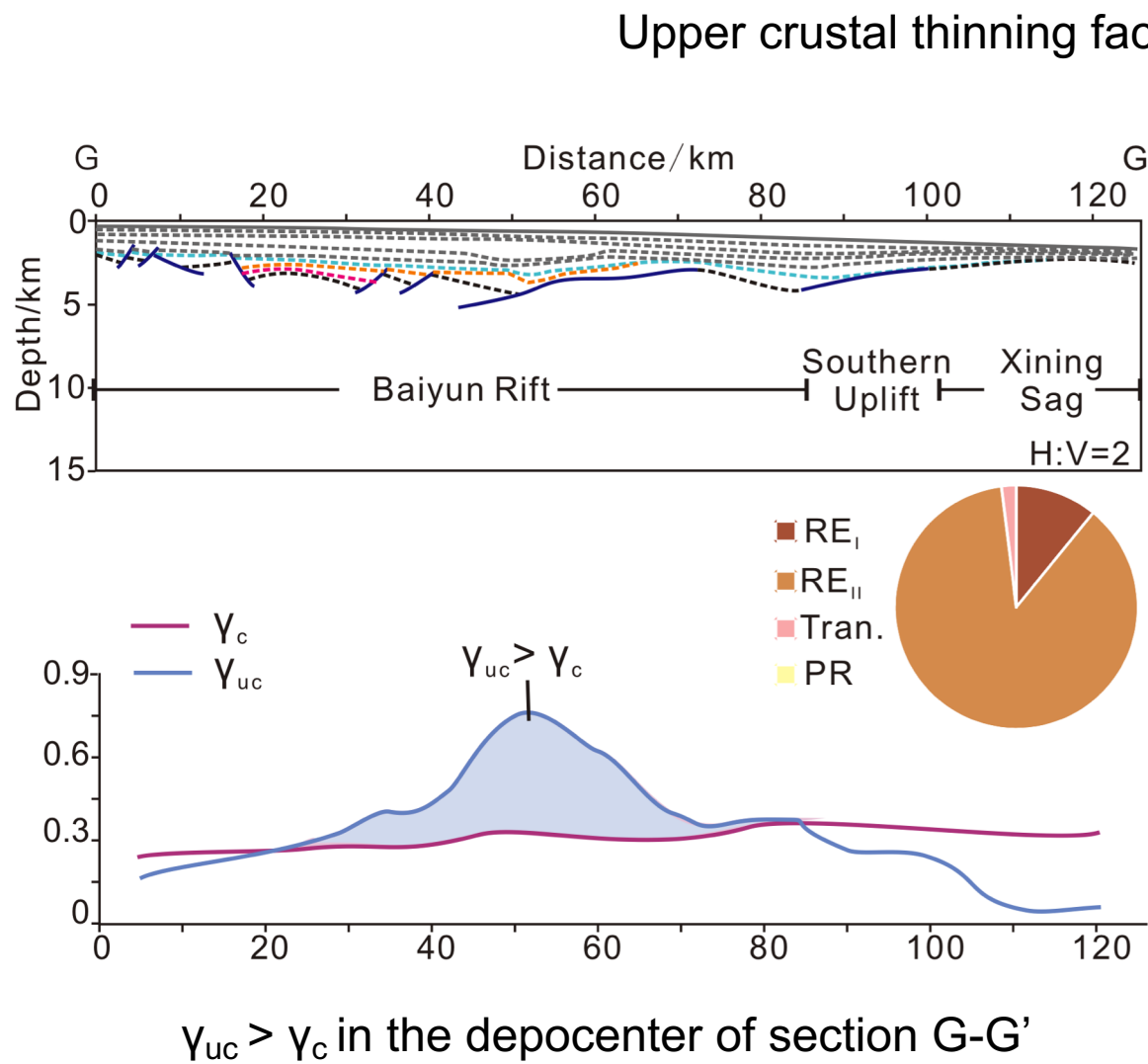
## Inverse discrepancy



Map compares the difference between  $\gamma_f$  and  $\gamma_c$

# Eastern Baiyun Rift

## Inverse discrepancy

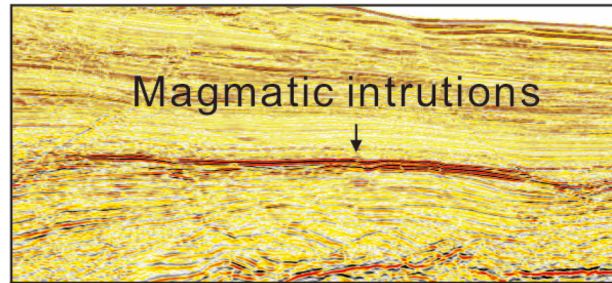


Map compares the difference between  $\gamma_{uc}$  and  $\gamma_c$

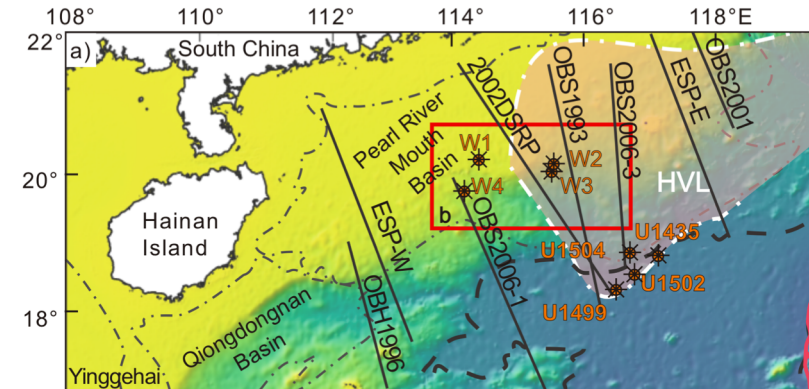
# Eastern Baiyun Rift

Possible cause: Lower crustal exhumation

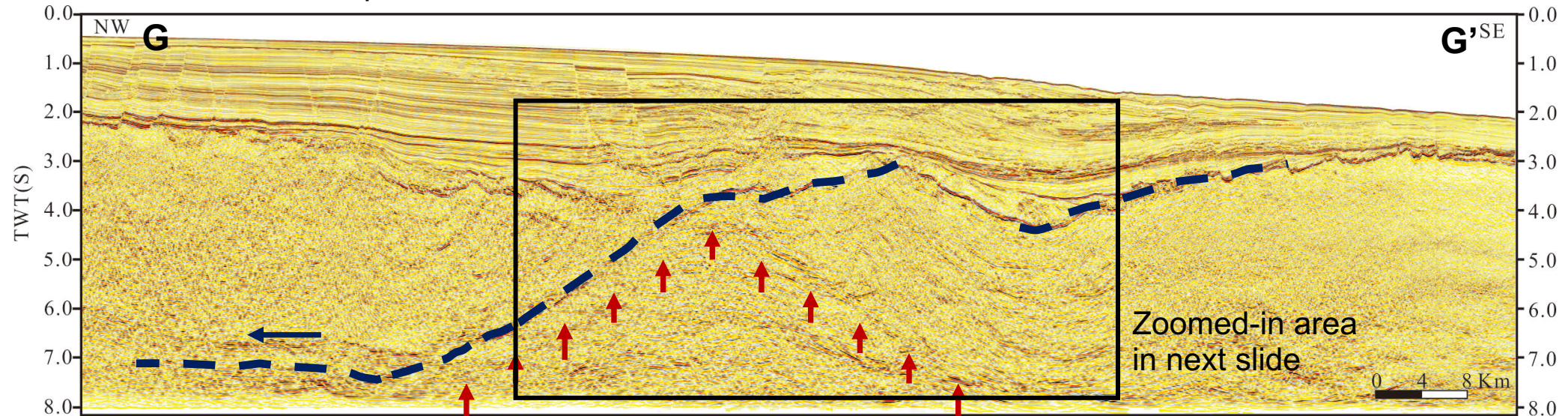
Evidence 1 More intense magmatism in the eastern Baiyun Rift (Zhao F. et al., 2016)



Evidence 2 High-velocity layer in the lower crust extending to the northeast along the NSCS (Yan et al., 2001; Wei et al., 2011)

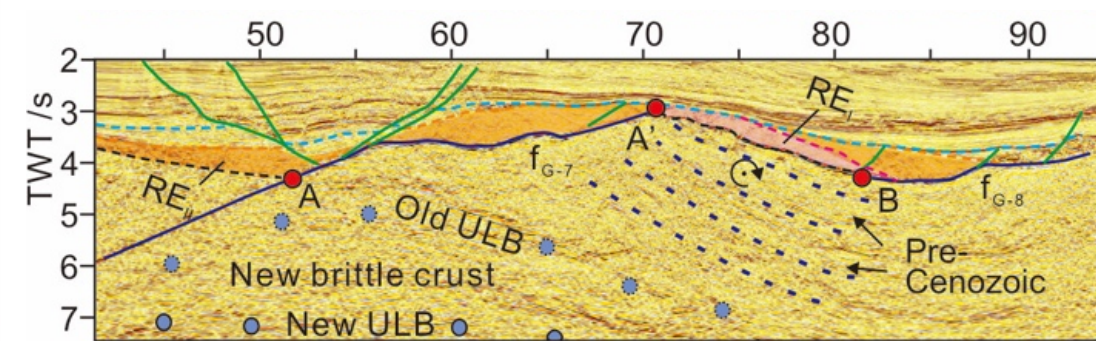
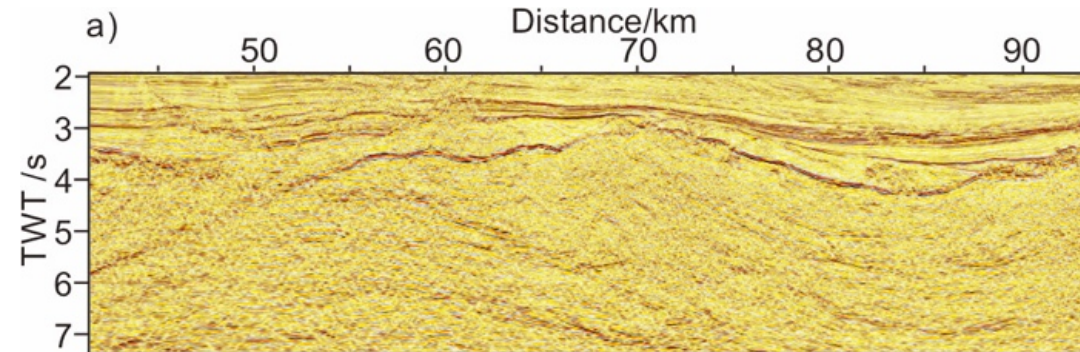


Evidence 3 A dome-shaped structure with chaotic internal reflections is in the footwall of the main LANFs

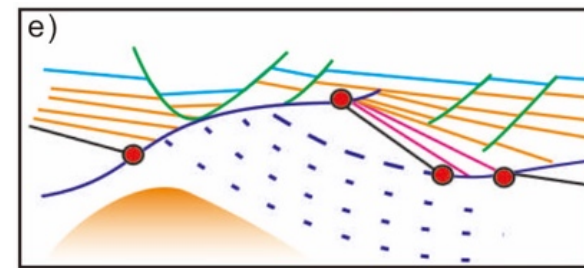
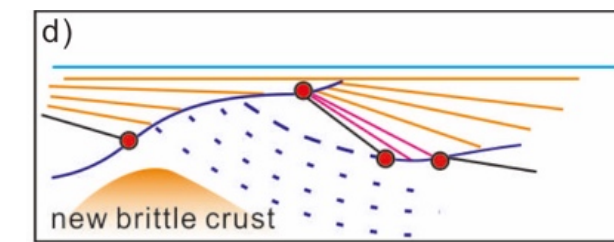
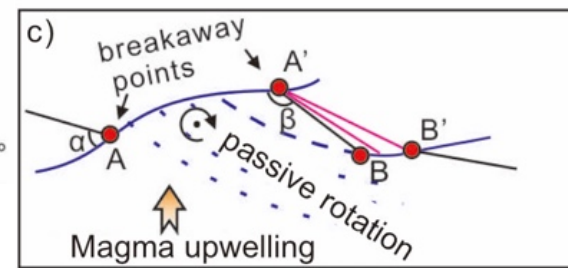
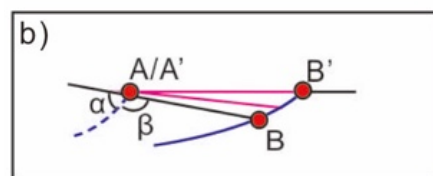


# Eastern Baiyun Rift

Polyphase detachment faulting caused the exhumation of the lower crust. Due to isostasy, the magma passively upwelled and thickened the crust and thus results in an underestimation of the whole crustal extension.



a) At least two phases of faulting with two couples of breakaway points, A/A' and B/B', are identified.



b) Sequential development of f<sub>G-7</sub> and f<sub>G-8</sub> hyper-stretched brittle crust.

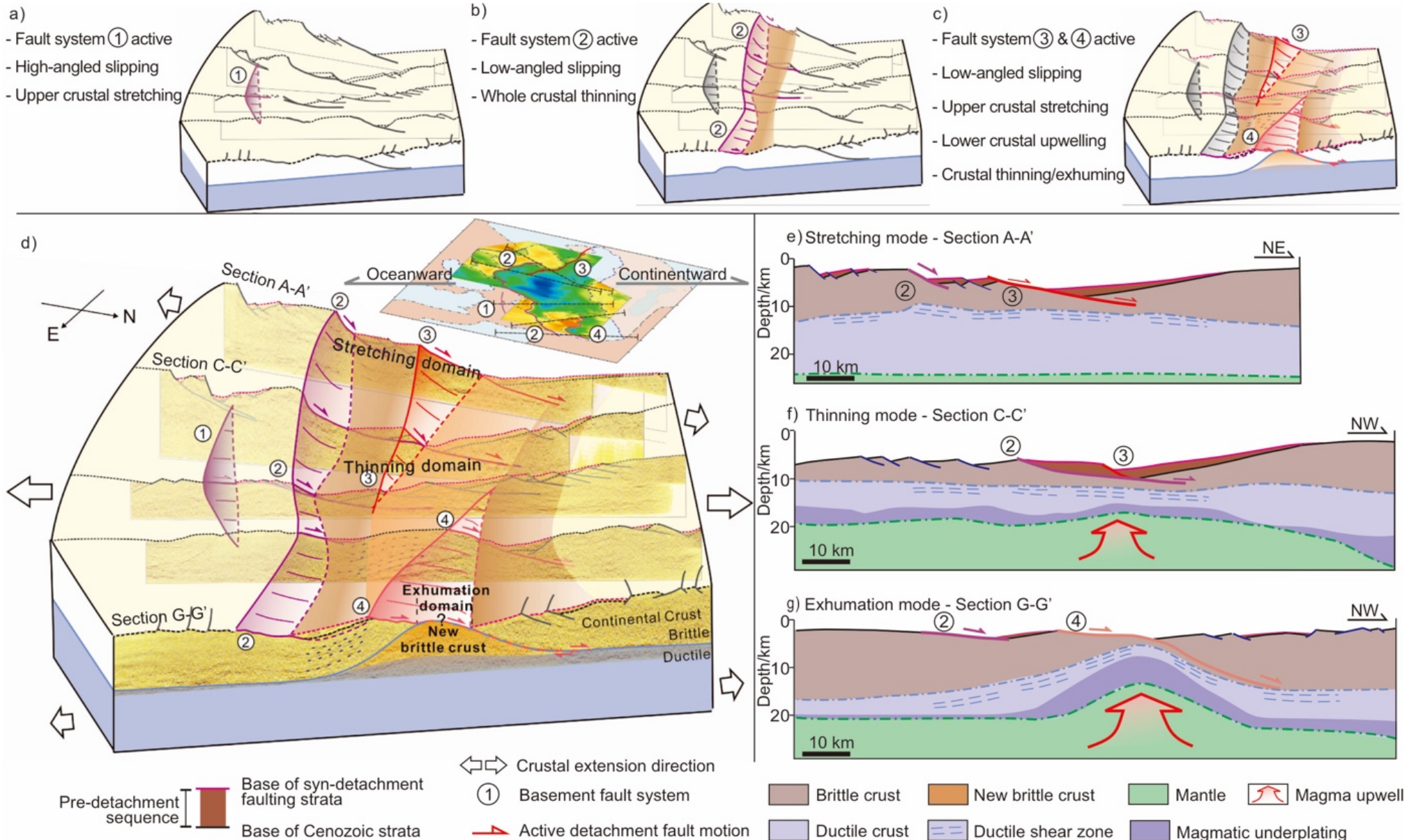
c) Due to isostasy, magmas migrated upward from the mantle, forming the dome-shaped structure at the footwall of the f<sub>G-7</sub>.

d) With the cooling of magmas, the ductile materials become brittle. New brittle crust and new ULB formed.

e) During post-rifting stage, faults re-activated while have not changed rift geometry.

# Summary

- Models of polyphase faulting leading to a later detachment faulting associated with a lower crustal exhumation in the eastern Baiyun Rift. See notes at end of presentation.



# Notes

---

## Slide # 10

Interpretations of sections A-A', C-C', E-E', and G-G' in time and depth domains. The pattern of the basement faults changes from a stair-step combination in the west, to a deformed singular fault with large displacements in the east. Shallow dipping basement faults sole out at a depth of 7s-8s TWT, where high-amplitude and continuous reflections developed. We interpret a brittle-ductile transition is at this depth. Moho depth is extracted from the previous result (Li et al., 2019). P-wave velocity is after Yan et al., (2001). RE<sub>I</sub>, rift episode I; RE<sub>II</sub>, rift episode II; Tran., transition stage; PR, post-rift stage.

In the west, basement faults are rooting at different depths, suggesting multiple decollement zones. ULB truncates SW-dipping reflections in the lower crust. In the east, a dome-shaped structure with chaotic internal reflections is in the footwall of the main LANFs. Parallel contacting relationship of the dome flank, pre-Cenozoic reflection and the hanging wall of the LANF suggests a synchronic deformation of these structures.

## Slide # 11

Error bars of  $\gamma_f$  indicate a range of 0-60% of extension which could be underestimated due to a sub-resolution faulting (Clift & Sun, 2006). Blue and orange shaded regions represent  $\gamma_{uc} > \gamma_c$  and  $\gamma_f > \gamma_c$ , indicating inverse discrepancy. Pie graphs demonstrate the proportion of the extension in each structural evolution episode. The light brown category in the pie graph has the largest proportion shows the most intense extension happened in the RE<sub>II</sub> when low-angled faults were active.  $\gamma_c'$  is the thinning factor of the whole crust under an assumption that 50% of the basement is pre-Cenozoic remnants. The actual thinning factor of the crust ranges from  $\gamma_c$  to  $\gamma_c'$ .

## Slide #19

(a-d) Block diagrams display a perspective view from the NE of the 3D volume, without sediments to expose the top of the acoustic basement. Four sets of the basement fault systems in the Baiyun Rift have been identified. These fault systems were initiated earlier in the central south and migrated to the NE and NW progressively.

(e-g) Models for temporal and spatial evolution of the hyper-thinning process based on observations from seismic sections in the Baiyun Rift. (e) Stretching mode is characterized by listric faulting, a differential subsidence of half-grabens, and a major ductile shear zone exemplified by section A-A', western Baiyun Rift. (f) Thinning mode is characterized by the maximum thinning of the crust and the presence of magmatic underplating in the lowest crust. (g) The exhumation mode is well documented by section G-G', eastern Baiyun Rift. This phase is distinguished by the exhumation and embrittlement of the lower crust from less than 5 km depth along a downward-concave fault ④.

# References

---

- Bai, Y., Dong, D., Brune, S., et al. (2019). Crustal stretching style variations in the northern margin of the South China Sea. *Tectonophysics*, 751, 1-12.
- Clift, P. D., & Sun, Z. (2006). The sedimentary and tectonic evolution of the Yinggehai-Song Hong basin and the southern Hainan margin, South China Sea: Implications for Tibetan uplift and monsoon intensification. *JGR*, 111(6), 1–28.
- Clift, P. D., Lin, J., & Barckhausen, U. (2002). Evidence of low flexural rigidity and low viscosity lower continental crust during continental break-up in the South China Sea. *MPG*, 19(8), 951–970.
- Davis, M., & Kusznir, N. (2004). Depth-Dependent Lithospheric Stretching at Rifting Continental Margins. In *Rheology and Deformation of the Lithosphere at Continental Margins* (pp. 92–137).
- Franke, D., Barckhausen, U., Baristeas, N., et al. (2011). The continent-ocean transition at the southeastern margin of the South China Sea. *MPG*, 28(6), 1187–1204.
- Hsu, S., Yeh, Y., Doo, W.-B., et al. (2004). New bathymetry and magnetic lineations identifications in the northernmost South China Sea and their tectonic implications. *MGR*, 25(1–2), 29–44.
- Huang, C., Zhou, D., Sun, Z., et al. (2005). Deep crustal structure of Baiyun Sag, northern South China Sea revealed from deep seismic reflection profile. *Chinese Science Bulletin*, 50(11), 1131–1138.
- Kusznir, N.J., Hunsdale, R., Roberts, et al. (2005). Norwegian margin depth dependent stretching, in Doré, A.G., and Vining, B.A., eds., *Petroleum geology: Northwest Europe and global perspectives—Proceedings of the 6th Petroleum Geology Conference*: Geological Society [London], Petroleum Geology Conferences Ltd., p. 767–783
- Li, F., Sun, Z., Pang, X., et al. (2019). Low-Viscosity Crustal Layer Controls the Crustal Architecture and Thermal Distribution at Hyperextended Margins: Modeling Insight and Application to the Northern South China Sea Margin. *G3*, 20(7), 3248–3267.
- Moulin, M., Aslanian, D., Olivet, J.-L., et al. (2005). Geological constraints on the evolution of the Angolan margin based on reflection and refraction seismic data (Zaïango project). *Geophysical Journal International*, 162(3), 793–810.
- Savva, D., Pubellier, M., Franke, D., et al. (2014). Different expressions of rifting on the South China Sea margins. *MPG*, 58(PB), 579–598.
- Tong, D., Ren, J., Lei, C., et al. (2009). Lithosphere Stretching Model of Deep Water In Qiongdongnan Basin, Northern Continental Margin of South China Sea, and Controlling of Post-Rift Subsidence. *Earth Science*, 34(6), 963–974.
- Wei, X., Ruan, A., Zhao, M., et al. (2011). A wide-angle OBS profile across Dongsha Uplift and Chaoshan Depression in the mid-northern South China Sea. *Chinese Journal of Geophysics*, 54(12), 3325–3335
- White, N., 1990, Does the uniform stretching model work in the North Sea?, in Blundell, D.J., and Gibbs, A.D., eds., *Tectonic evolution of the North Sea rifts: International Lithosphere Program Publication 181*, p. 217–239.
- Yan, P., Zhou, D., Liu, Z. (2001). A crustal structure profile across the northern continental margin of the South China sea. *Tectonophysics*, 338(1), 1–21.
- Zhao, F., Alves, T. M., Wu, S., et al. (2016). Prolonged post-rift magmatism on highly extended crust of divergent continental margins (Baiyun Sag, South China Sea). *EPSL*, 445(July), 79–91.
- Zhao, Y., Ren, J., Pang, X., et al. (2018). Structural style, formation of low angle normal fault and its controls on the evolution of Baiyun Rift, northern margin of the South China Sea. *MPG*, 89, 687–700.
- Zhao, Z., Sun, Z., Liu, J., et al. (2018). The continental extension discrepancy and anomalous subsidence pattern in the western Qiongdongnan Basin, South China Sea. *EPSL*, 501, 180–191.
- Ziegler, P.A., 1983, Crustal thinning and subsidence in the North Sea: Comment: *Nature*, 304, 561.

*THANK YOU*

Email: [zhaoyh@sio.org.cn](mailto:zhaoyh@sio.org.cn)